

Recent Improvements in Radar Techniques for Investigating the Upper Atmosphere



Iain Reid ^{[1],2}

Joel Younger¹, Robert A. Vincent¹, David A. Holdsworth^{1,2} and Daniel McIntosh¹

¹School of Chemistry and Physics, University of Adelaide, Adelaide, Australia

²ATRAD Pty Ltd, Thebarton, South Australia, Australia,

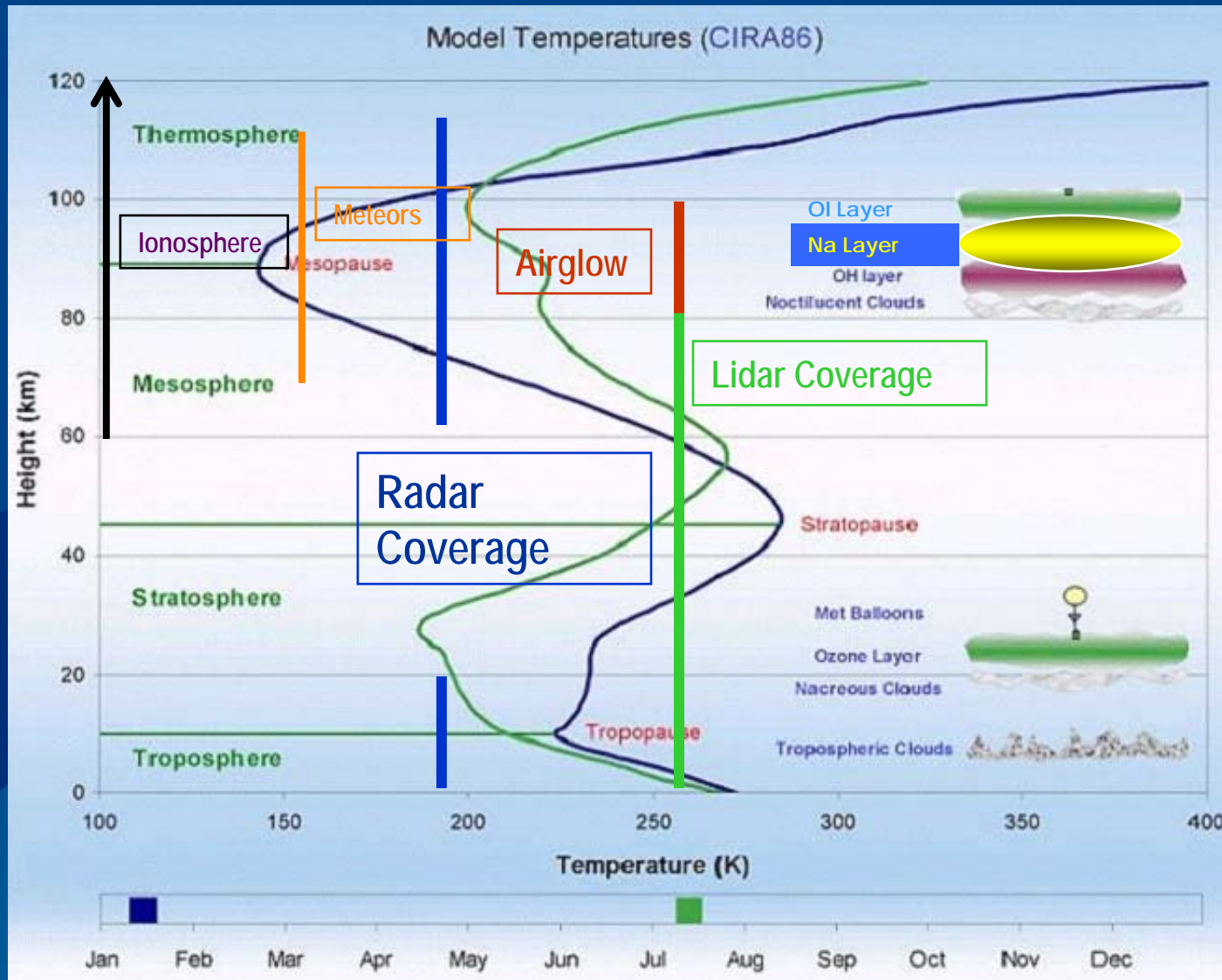
^[1] Email: iain.reid@adelaide.edu.au



SuperDARN 2008 Annual Meeting
Newcastle, NSW. Australia
1st – 6th of June 2008



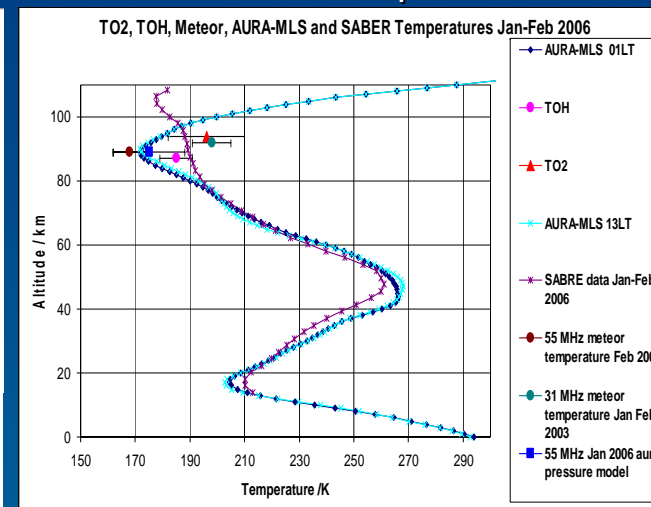
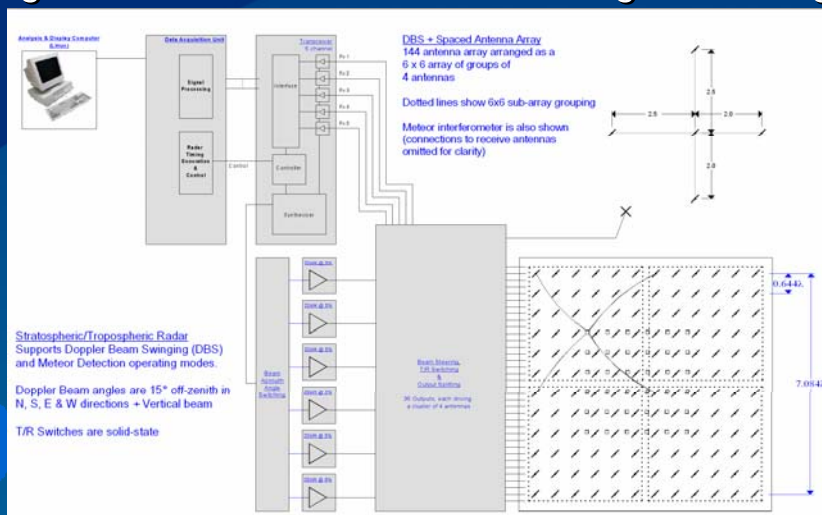
The Atmosphere below 120 km



The
Mesosphere
Lower
Thermosphere
(MLT) region
(50-110 km)

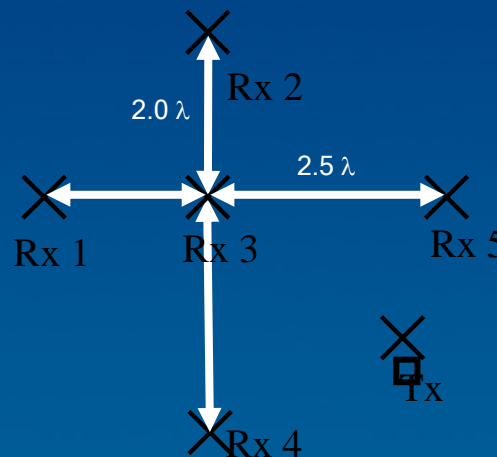
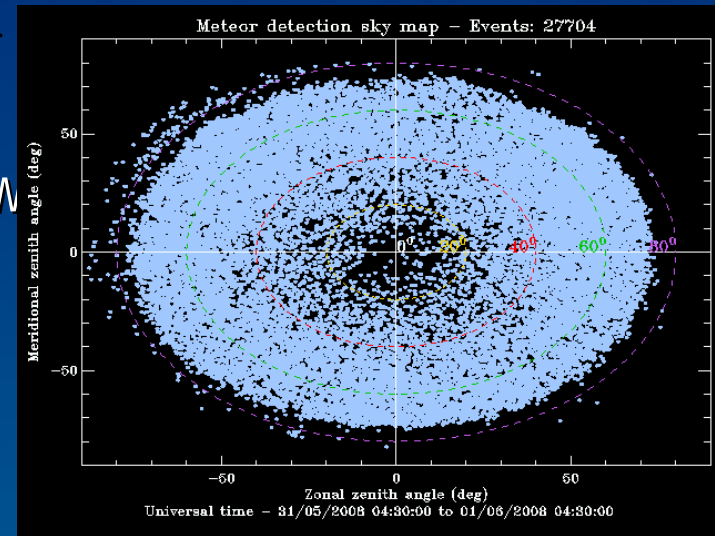
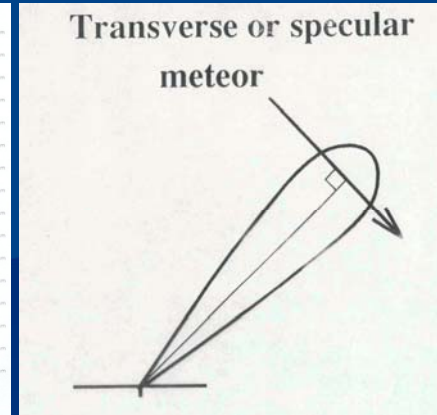
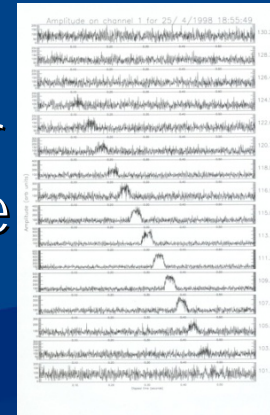
Meteor Radar

- The most significant recent improvements have occurred around the “re-birth” of the meteor radar technique for investigating the MLT region of the atmosphere
- Two techniques:
 - Narrow-beam radar. Source of “re-birth” but now less commonly used. Originally applied on stratospheric tropospheric (ST) radar, and now also ISR
 - All-sky method with interferometer to locate meteor trail
- Line-of-sight velocities measured from Doppler shift of trail
- Atmospheric temperatures estimated from diffusion of trail. Important because global models indicate a cooling of the region with lower atmosphere warming



Meteor Radar

- While more power can be put into a given solid angle with a narrow beam radar, thus increasing the detectability of "faint" meteor trails, increasing the angle illuminated more than compensates for this and counts are generally better with all-sky systems
- Furthermore, the atmosphere as a detector favours lower look angles, and so all-sky illumination is now also pursued with narrow beam capable radars (as we will see shortly)



Examples of Meteor Trails



This image shows a meteor trail photographed by an astronomical telescope (incidentally).



This image shows a meteor smoke trail photographed at dusk

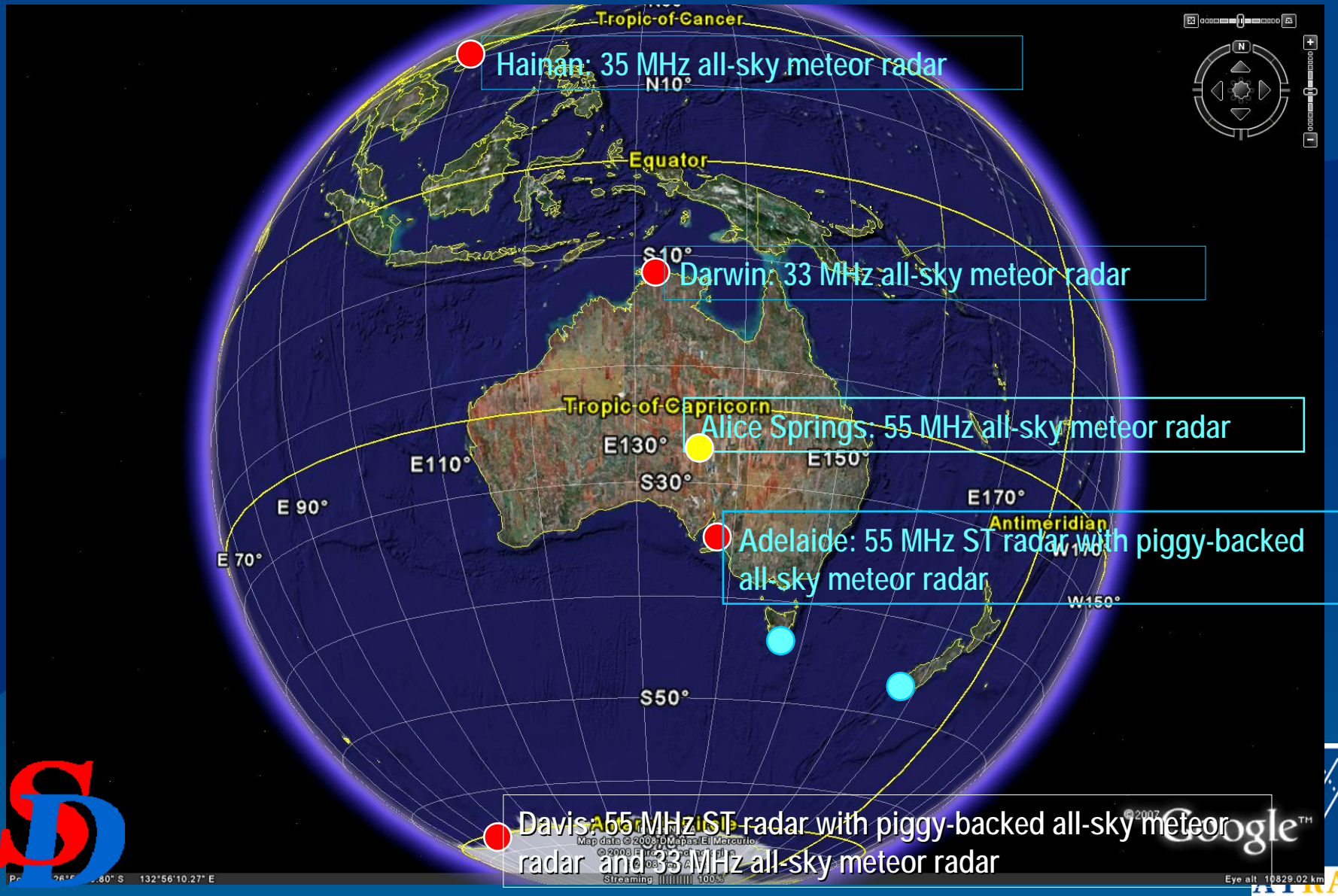


This image shows a photograph of a rocket trail. Note complex distortion by background wind.

The trail drifts with the background wind, and this can be used to measure wind velocity
The trail diffuses, and this can be used to estimate temperature



Selected Meteor Radar Locations



Radar Locations

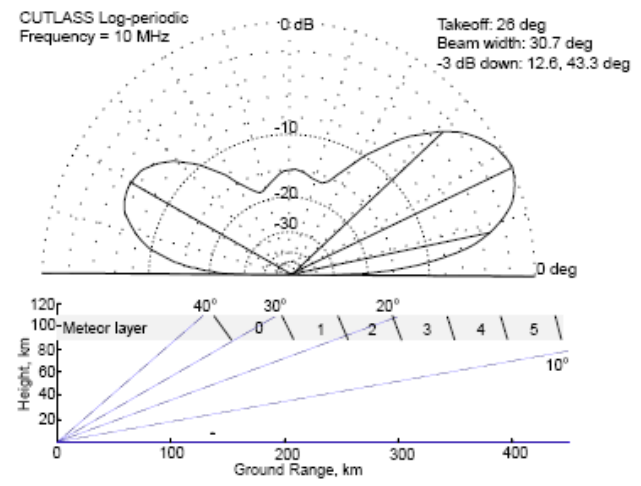
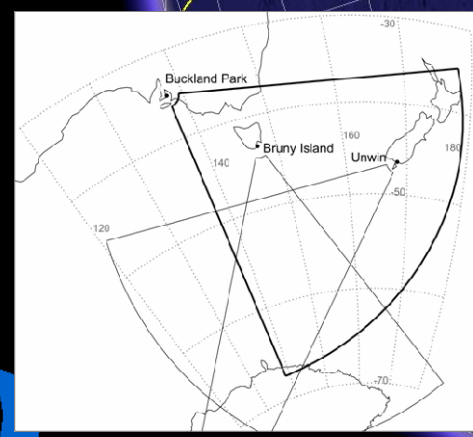
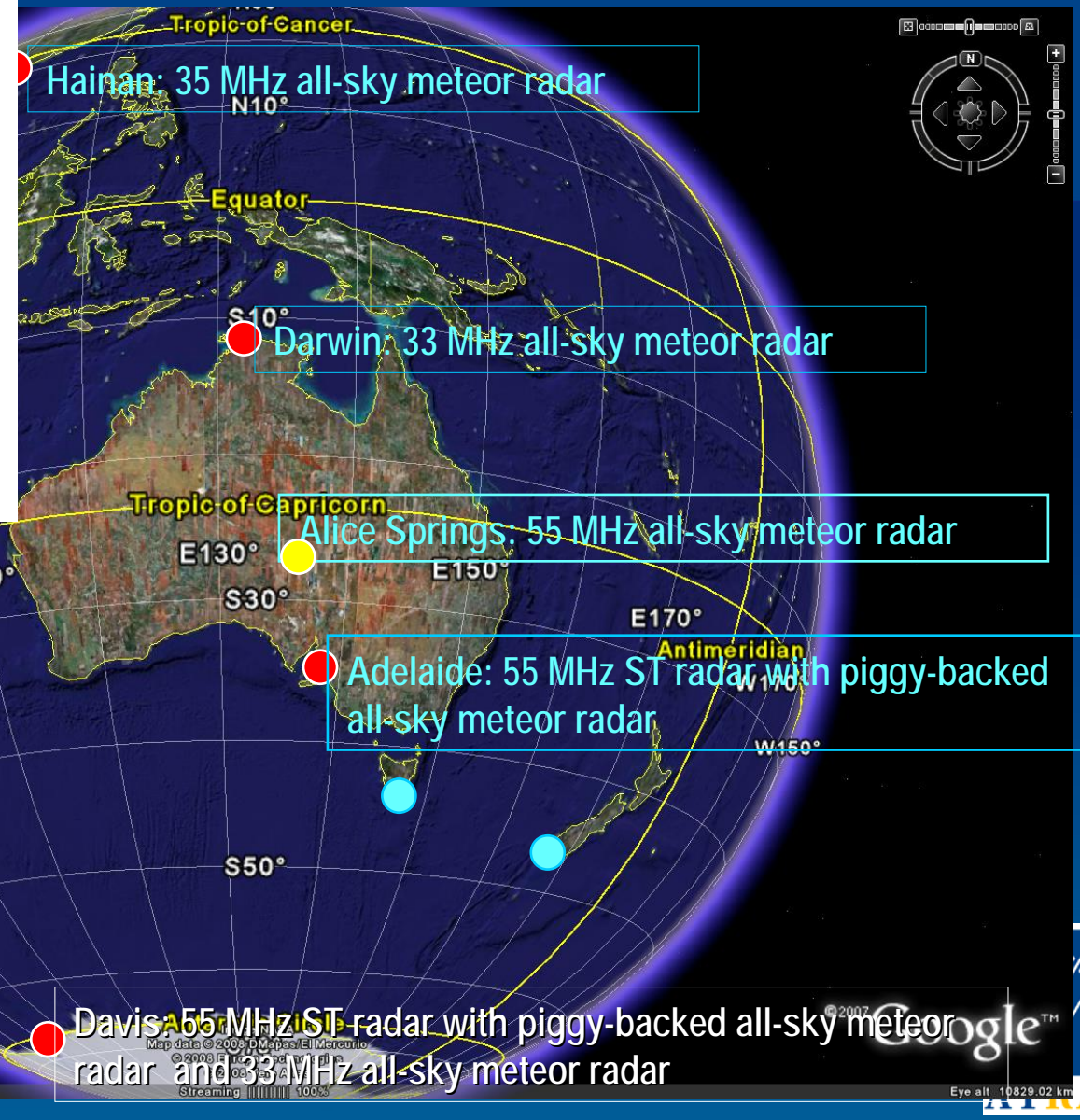


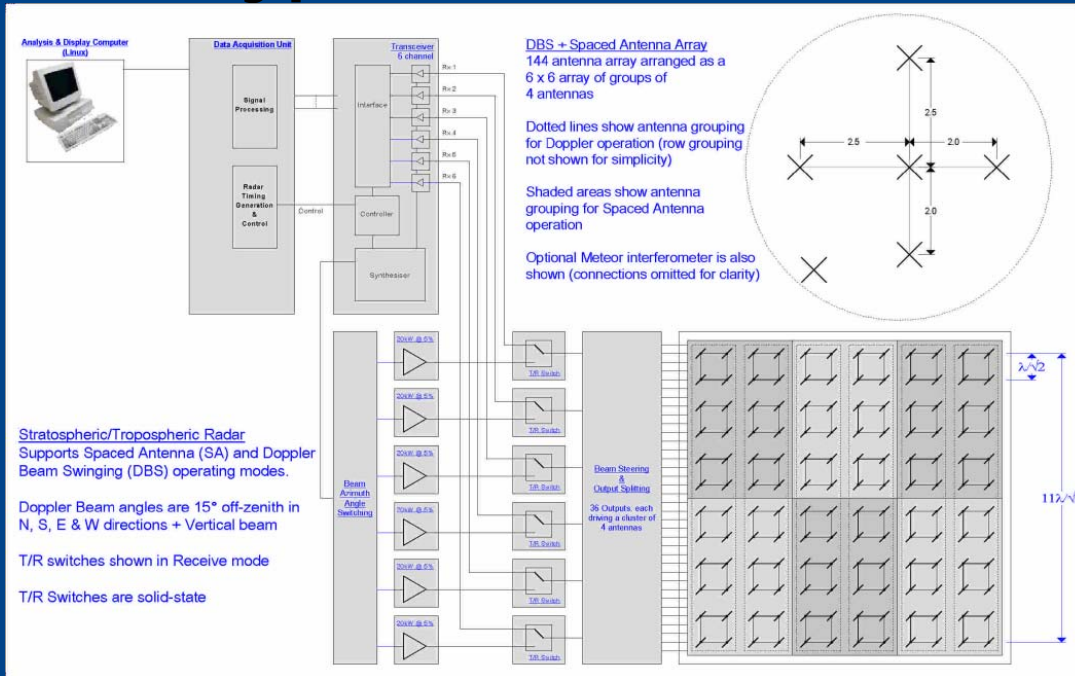
Fig. 1. (a) Log-periodic plot of the theoretical gain of the 10 MHz CUTLASS radar transmitter as a function of elevation angle for optimum azimuthal pointing direction. Maximum gain has a take off angle of 26° with a beam width of 30.7. (b) Intersections between the meteor ablation layer between 90–110 km and the six nearest SuperDARN range gates. Guide elevation angles in intervals of 10° are denoted by dashed lines.



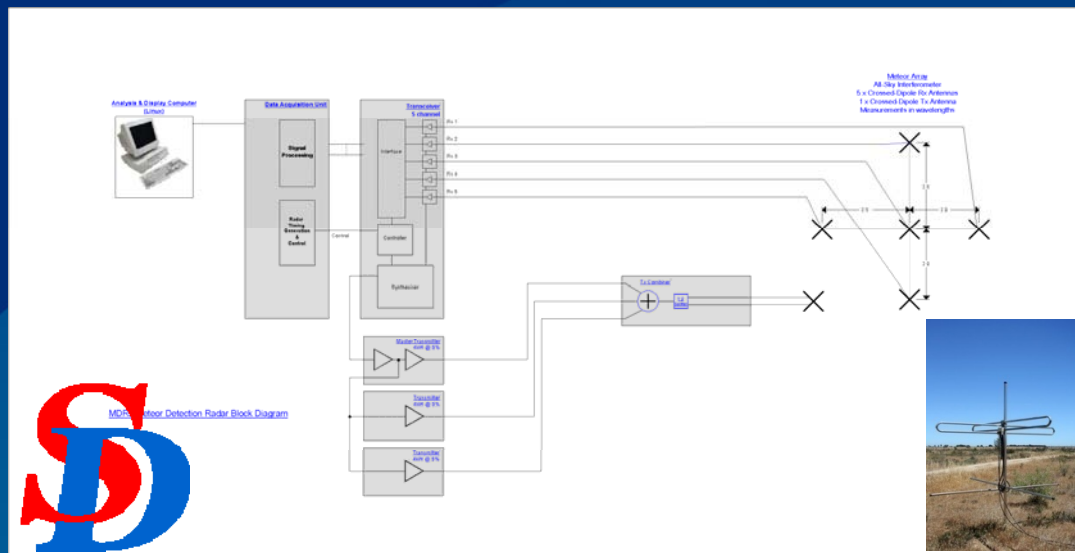
Buckland Park and existing TIGER radars



Two types of meteor radar used



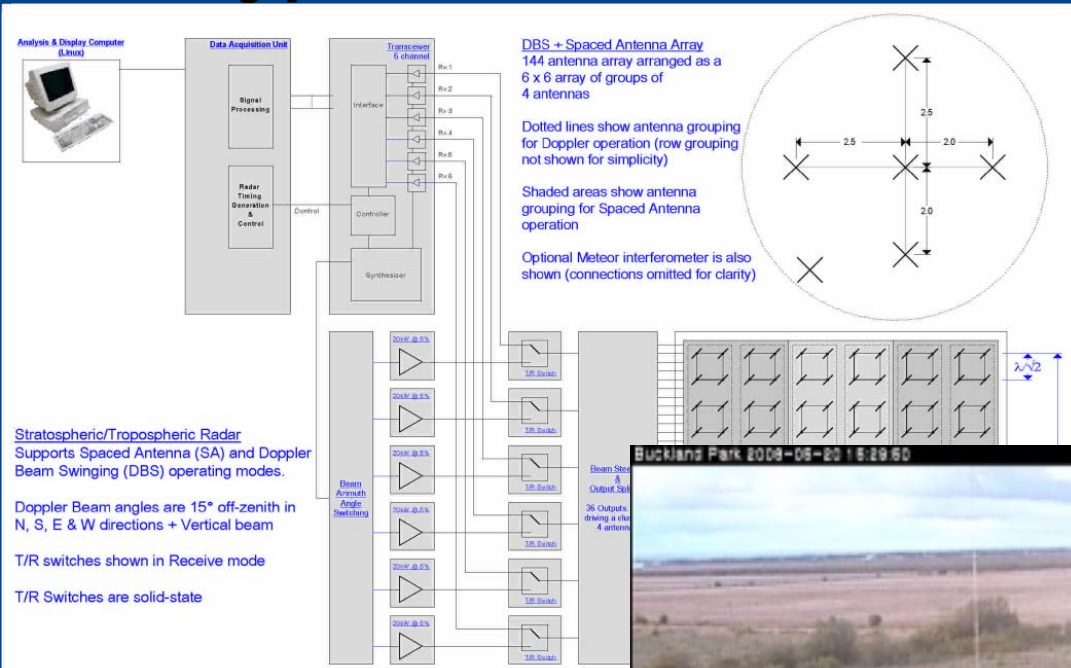
Interferometer piggy backed onto an ST radar (55 MHz). Incompatible operation, so interleaved



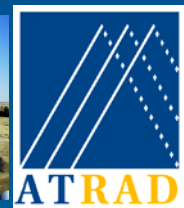
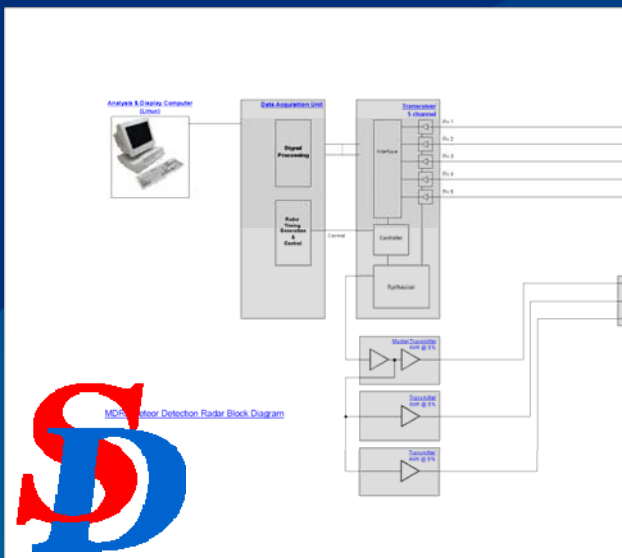
Dedicated all-sky meteor radar (near 30 MHz)



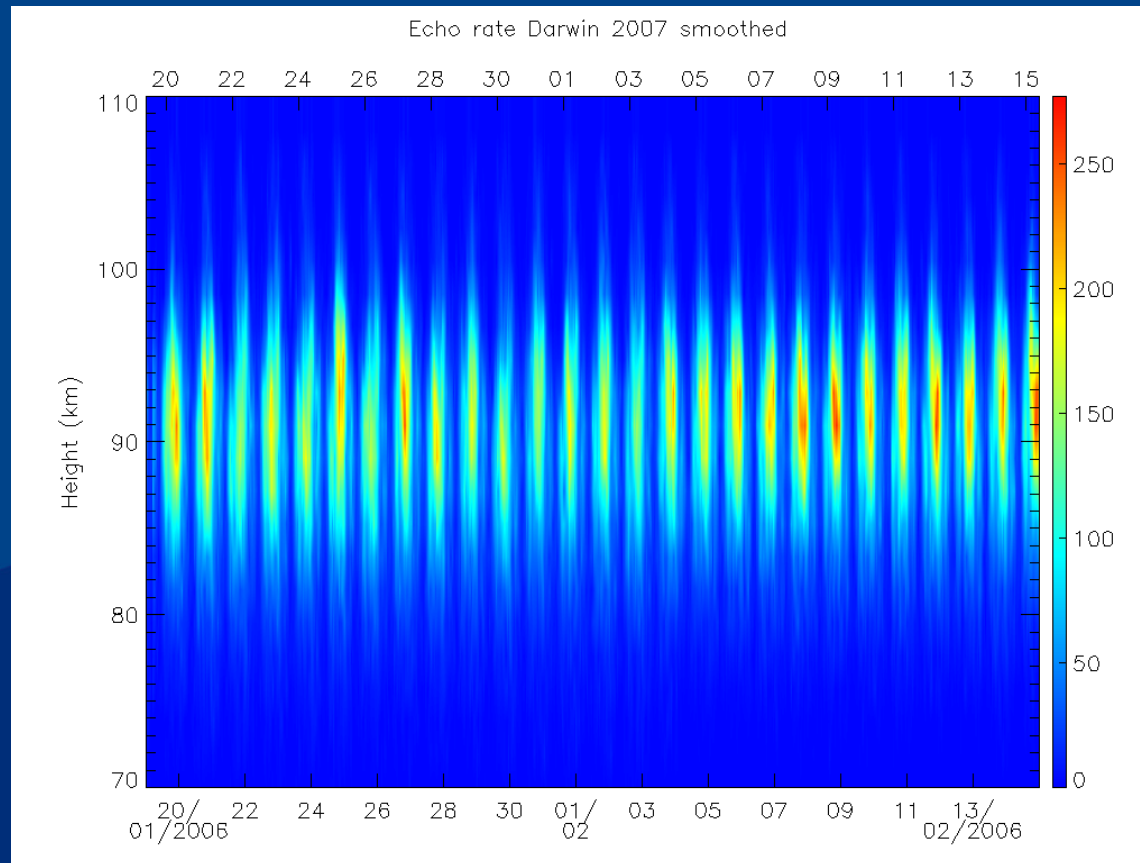
Two types of meteor radar used



Interferometer piggy backed onto an ST radar (55 MHz). Incompatible operation, so interleaved



Meteor radar performance: Darwin



Geometry strong
determinate in
sampling response

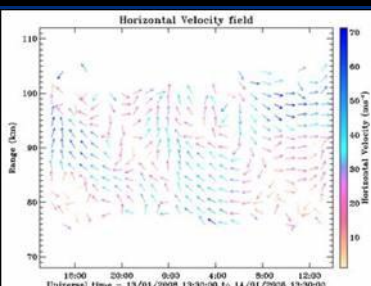
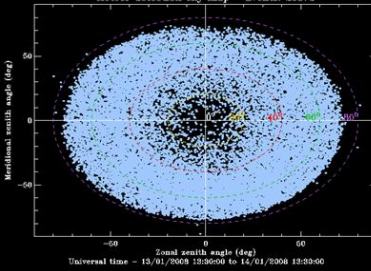
Note that these meteor
radar interferometers
are self-calibrating
using the meteor
echoes themselves



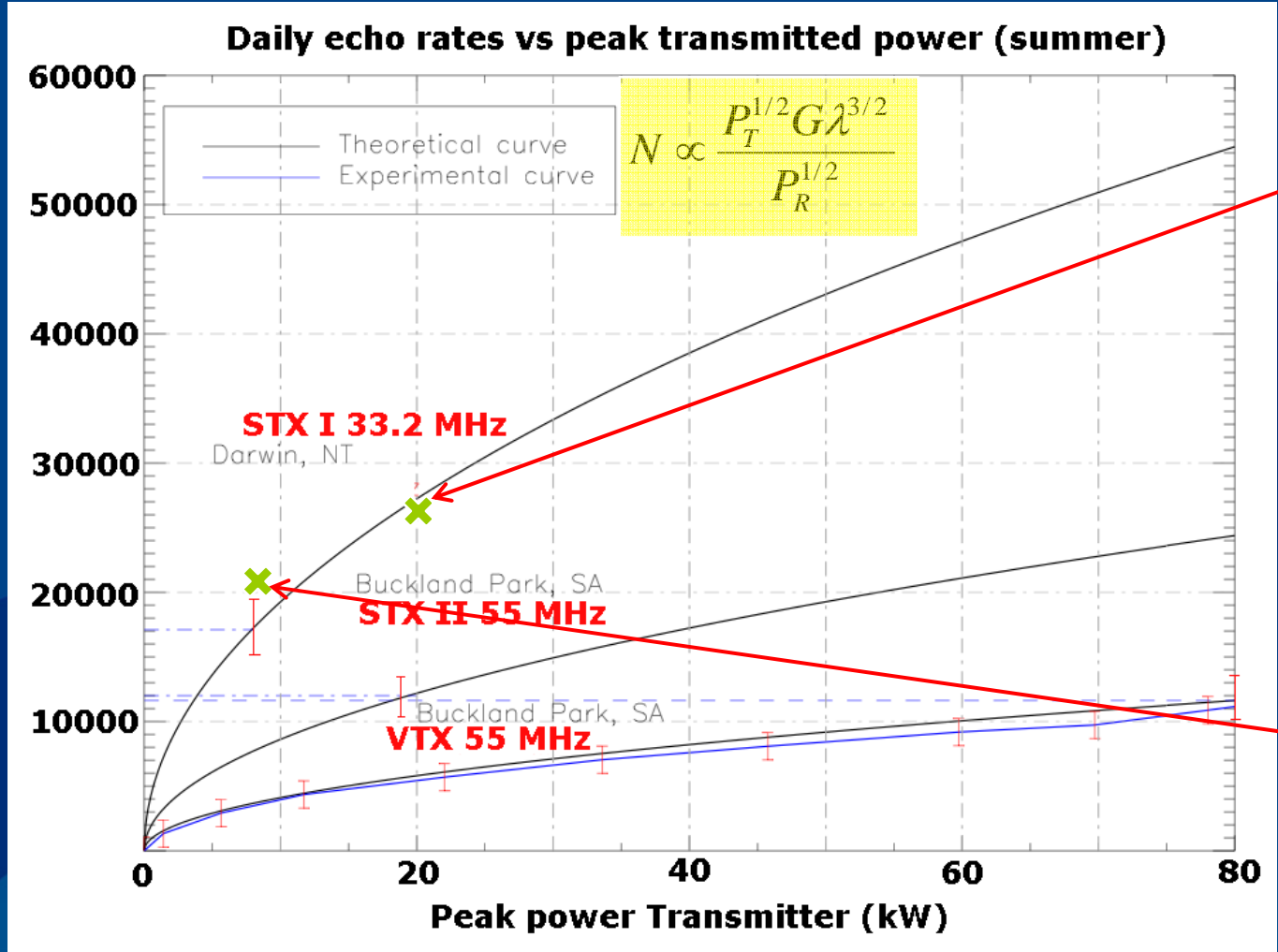
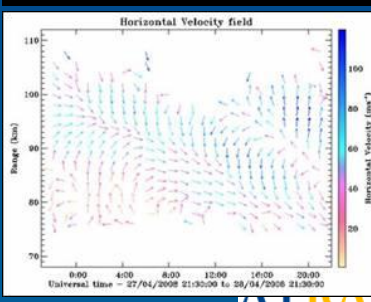
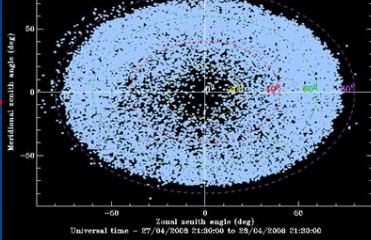
Meteor Radar Performance



Hainan Island



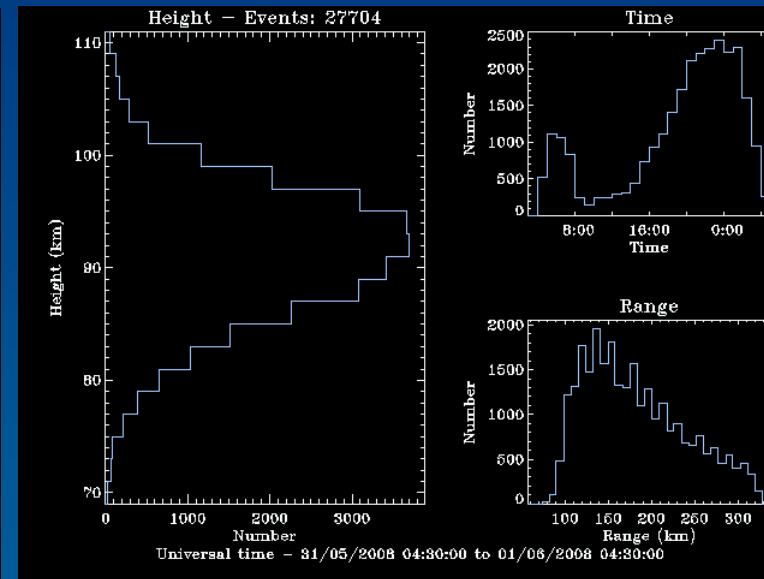
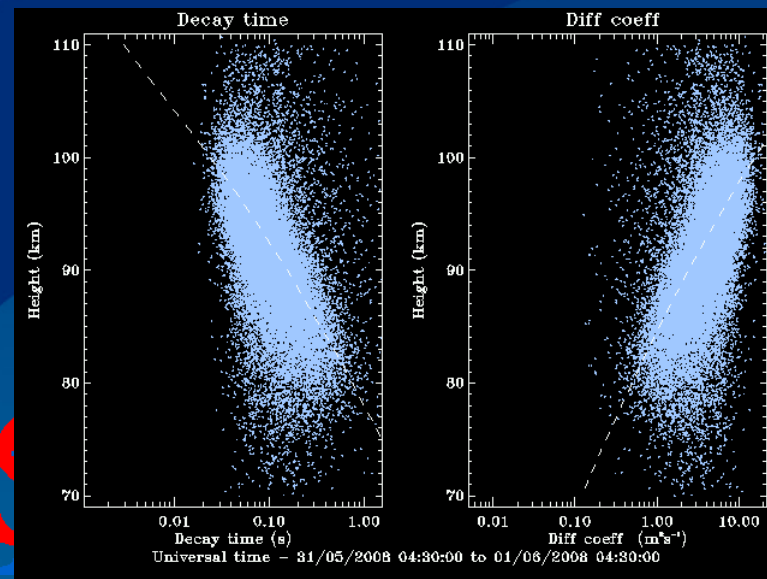
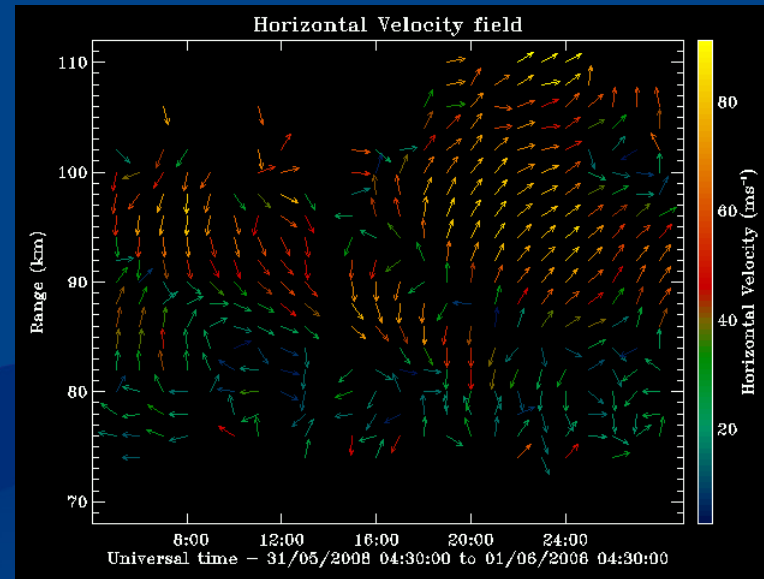
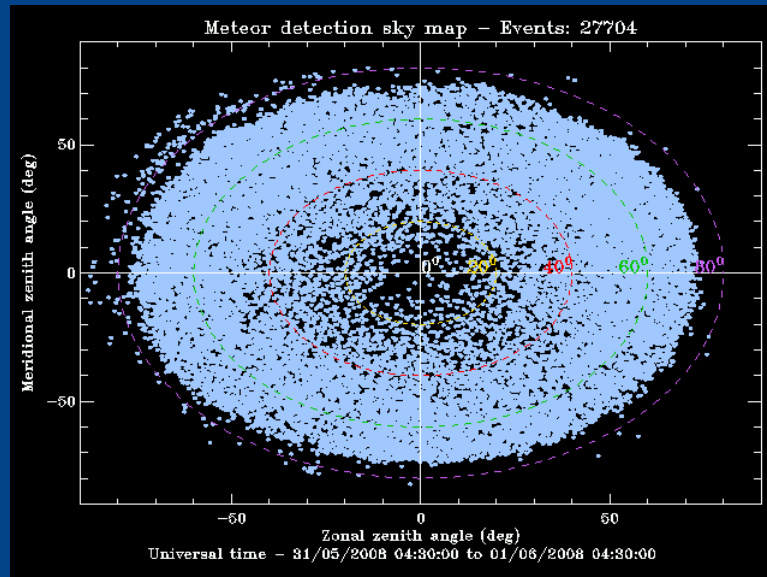
King George Island



Meteor counts versus radar power

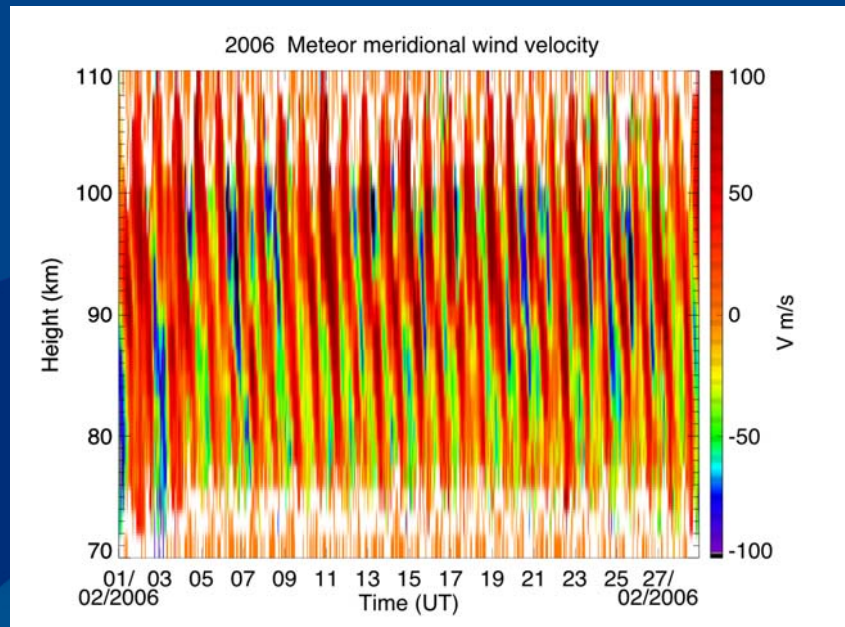
Observed (red error bar) meteor counts and McKinley's estimate (blue line) for various radar transmit powers

Typical results: one day

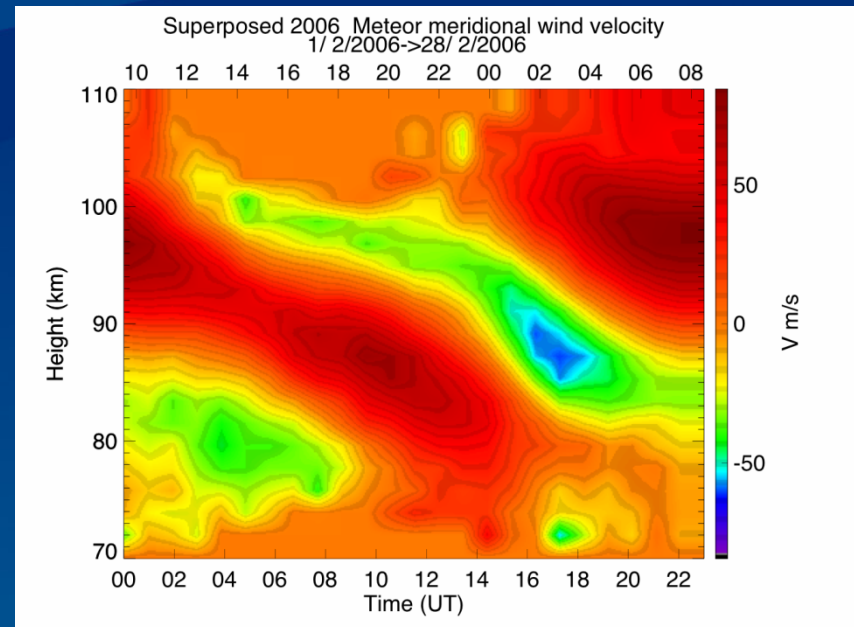


Typical results one month: Darwin

Meridional wind velocity

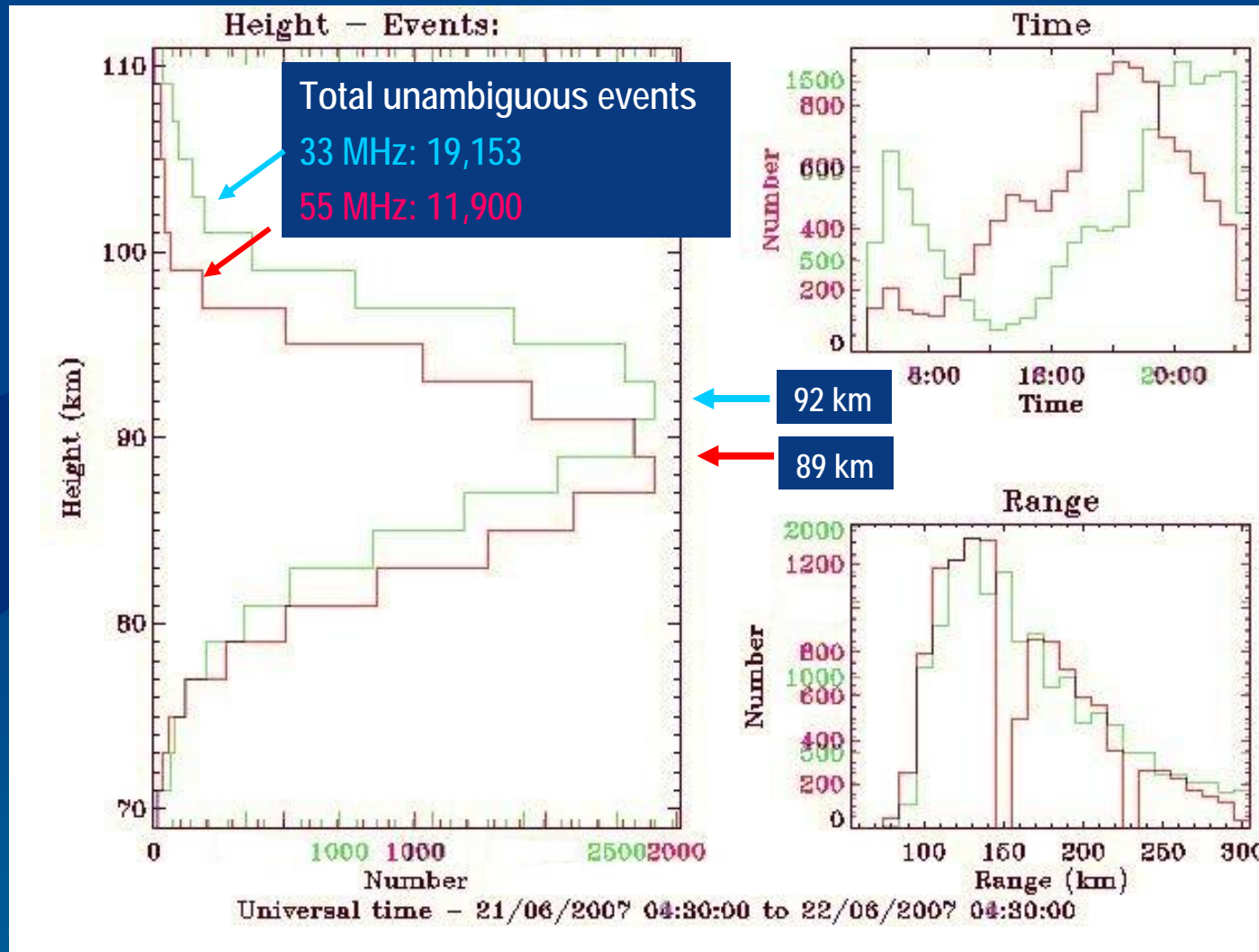


Superposed meridional wind



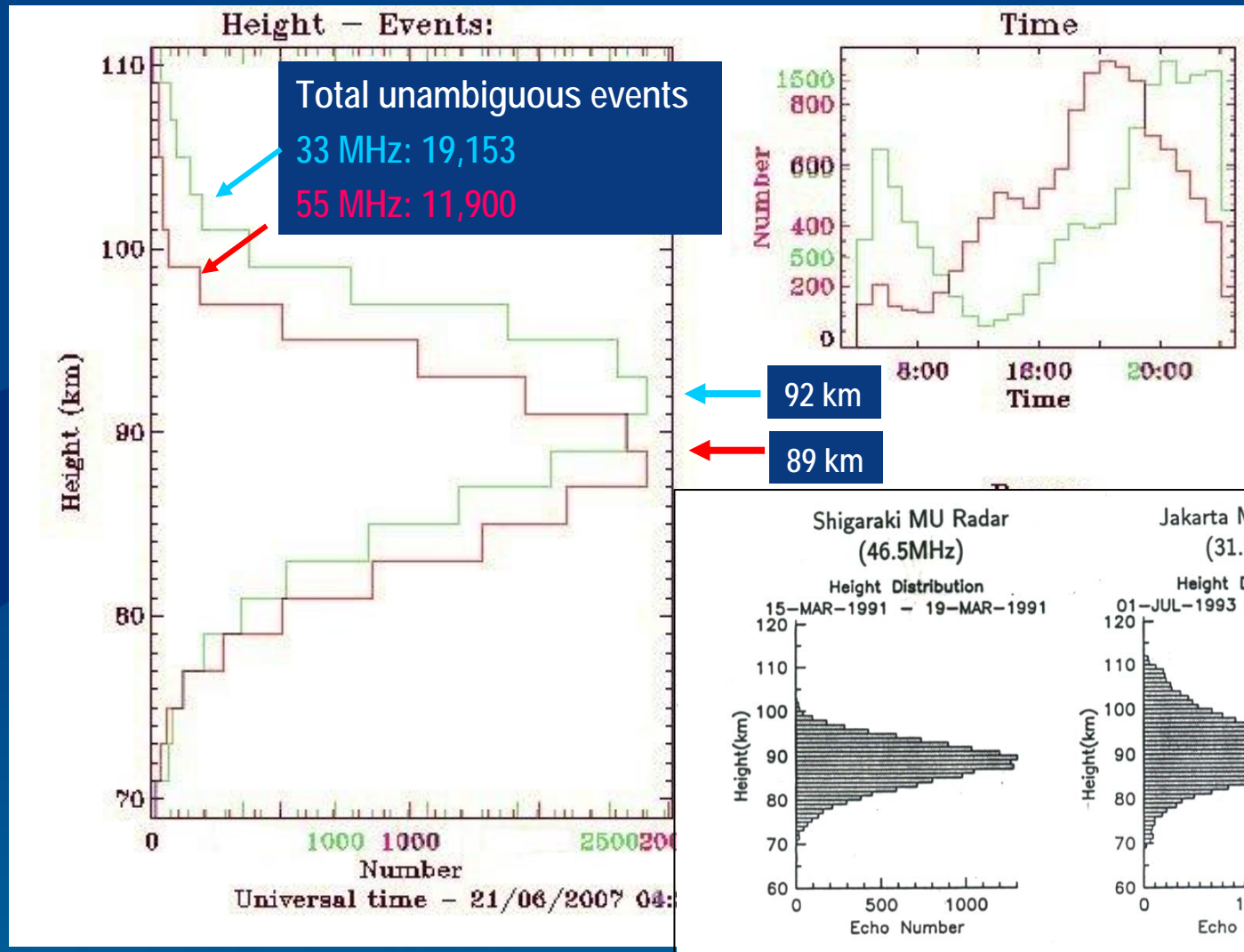
Meteor distributions at 55 (BP) and 33 MHz (Darwin) – typical day

The lower the frequency, the higher the peak of the distribution e.g., 2 MHz ~ 105 km



Meteor distributions at 55 (BP) and 33 MHz (Darwin) – typical day

The lower the frequency, the higher the peak of the distribution e.g., 2 MHz ~ 105 km



Meteor distributions

- There are few techniques to measure the neutral wind above 100 km. Previous observations of MF meteor winds (e.g., Tsutsumi et al., 1999) suggest great potential at HF
- However, quite challenging to discriminate meteor and ionospheric echoes at lower frequencies
- Anomalous diffusion becomes more important at heights above about 90 km
- Not aware of any meteor radars in the lower to mid HF band, but counts would be good, and height distribution would peak near 100 – 105 km
- Meteors with a low ablation-temperature would occur in the 100 - 140 km height region

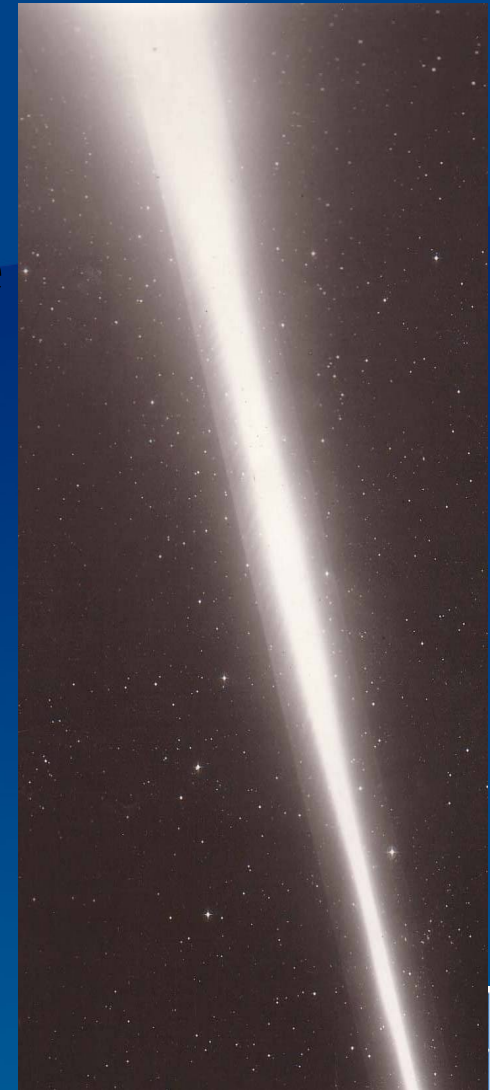
Trail diffusion

- McKinley (1961) showed the amplitude of the scattered radiation from the trail is given by

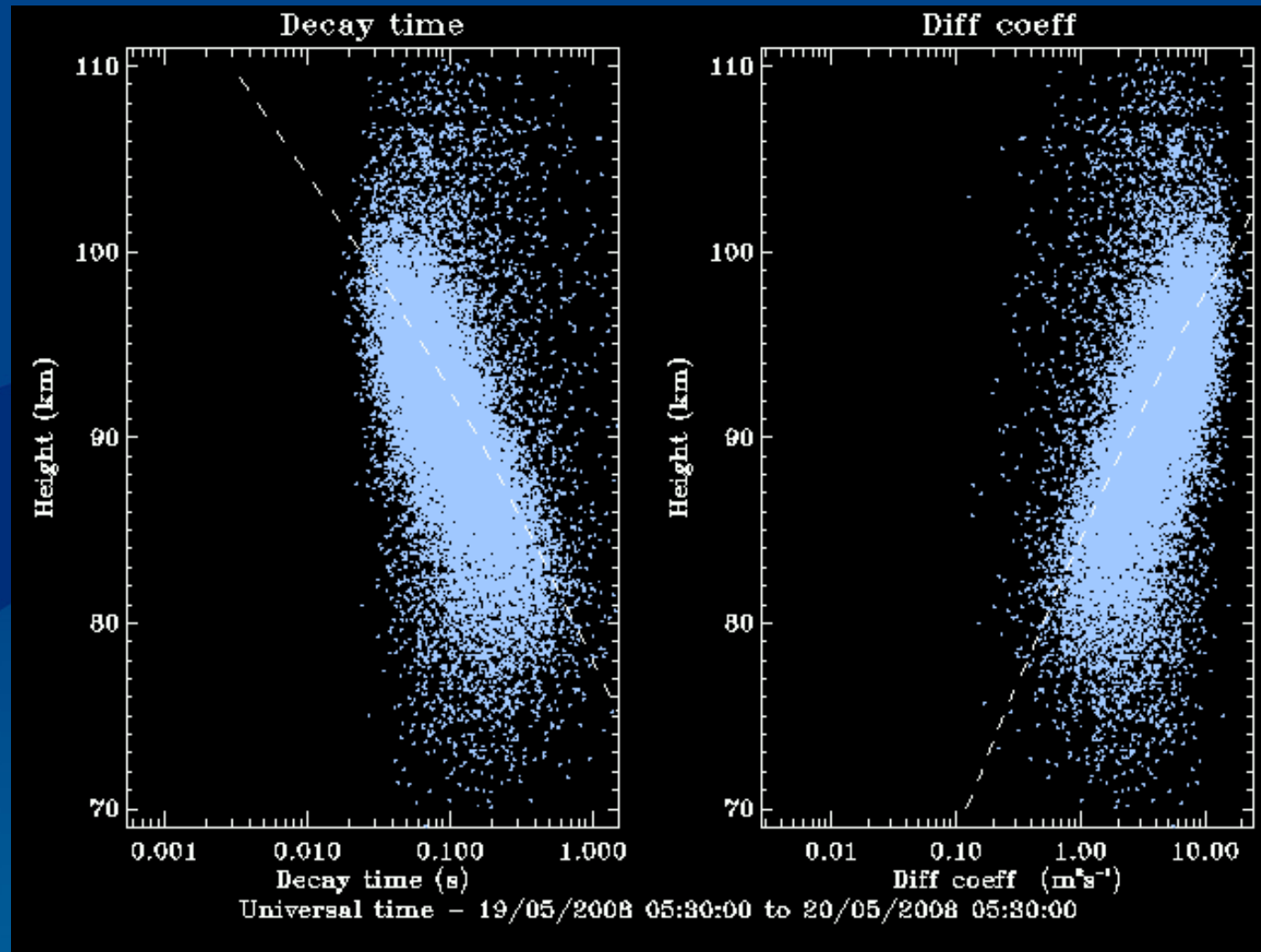
$$A \propto 2\pi \int_0^{\infty} n_e(r, t) r J_0\left(\frac{4\pi r}{\lambda}\right) dr$$

- And the diffusion of the trail is given by

$$\frac{\partial n_e(r, t)}{\partial t} = D \nabla^2 n_e(r, t)$$



Decay times and diffusion: typical day



Trail diffusion (continued)

- It follows that the decay time τ of an underdense meteor echo (with an initially Gaussian distribution) is given by

$$\tau = \frac{\lambda^2}{16\pi^2 D} \quad (1)$$

where λ is the radar wavelength, and D is the ambipolar diffusion coefficient [e.g. *Cervera and Reid, 2000*] and

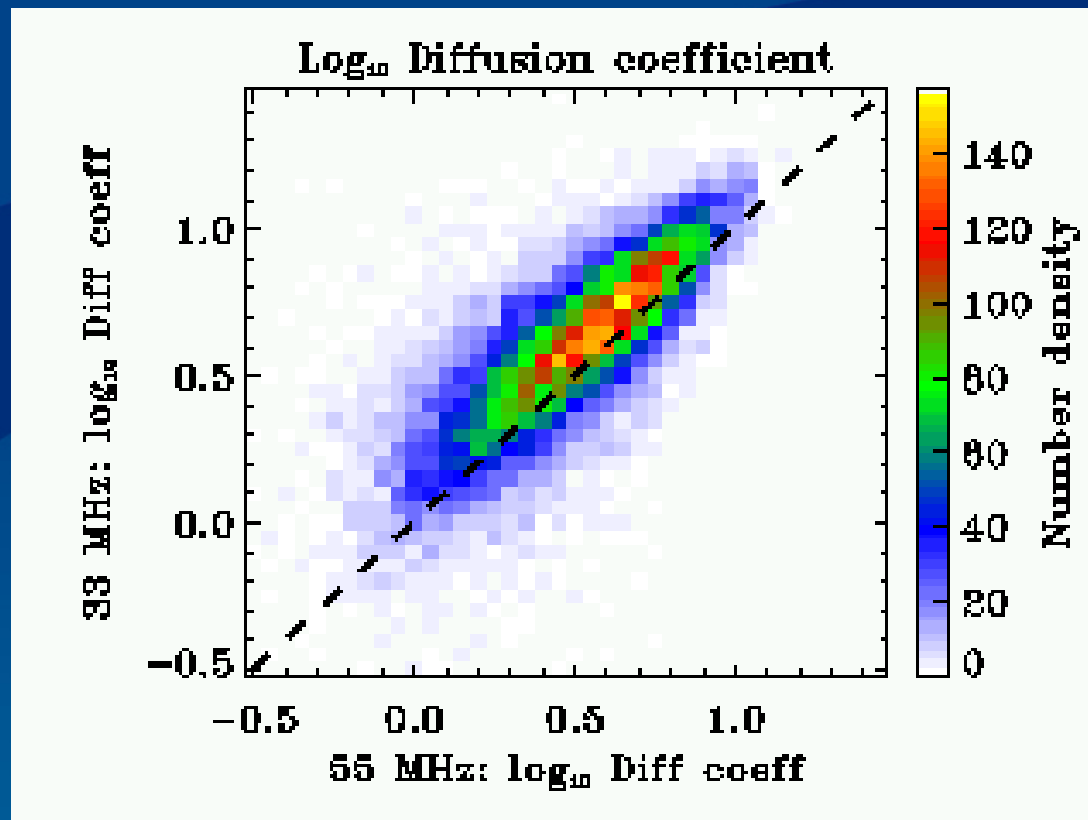
$$D = 6.39 \times 10^{-2} K_0 \frac{T^2}{P} \quad (2)$$

where K_0 is the zero field reduced mobility factor.



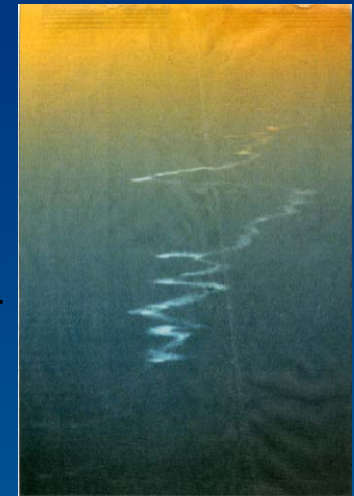
But....

- Diffusion coefficients calculated from the same meteors observed at 33 and 55 MHz at Davis Station, Antarctica are different



And...

- A dependence of trail diffusion on meteor echo power has also been observed by Singer et al., (2008)
- A similar dependence of the diffusion coefficient on echo power has been noted by Phil Chilson (private communication, 2007).
- Recall photo of meteor smoke trail, and consider what effect meteoric dust may have on trail diffusion:



Singer, W., Latteck, R., Millan, L. F., Mitchell, N. J. Fiedler (2008), Radar backscatter from Underdense Meteors and Diffusion Rates, *Earth Moon Planet*, 102, 403–409



Trail diffusion in the presence of dust



- Havnes and Sigernes (2005) suggested a model to account for the dependence of the diffusion rate in the presence of meteoritic dust. In this case, with R_{ed} as the electron capture rate of dust particles, and n_d the density of dust particles, the diffusion of the trail is given by

$$\frac{\partial n_e(r, t)}{\partial t} = D \nabla^2 n_e(r, t) - n_e(r, t) n_d(r, t) R_{ed}$$

- This equation has no analytic solution and must be handled numerically. Jones (1995) considered a non-Gaussian initial distribution of ionization about the trail axis and found that the Fourier transform of the density distribution of the trail decays exponentially with time, regardless of the shape. This can be exploited in an iterative solution

$$n_e(r, t + \Delta t) = \int_0^{\infty} sa(s, t) e^{-Ds^2 \Delta t} J_0(sr) ds - n_e(r, t) n_d(r, t) \Delta t$$

- Where $a(s, t)$ the Fourier transform of $n_e(r, t)$. The integral calculates the diffusion of a radially symmetric trail deformed by absorption over a small time step Δt . The term being subtracted is a linear estimate of the free electrons absorbed over the same time step.

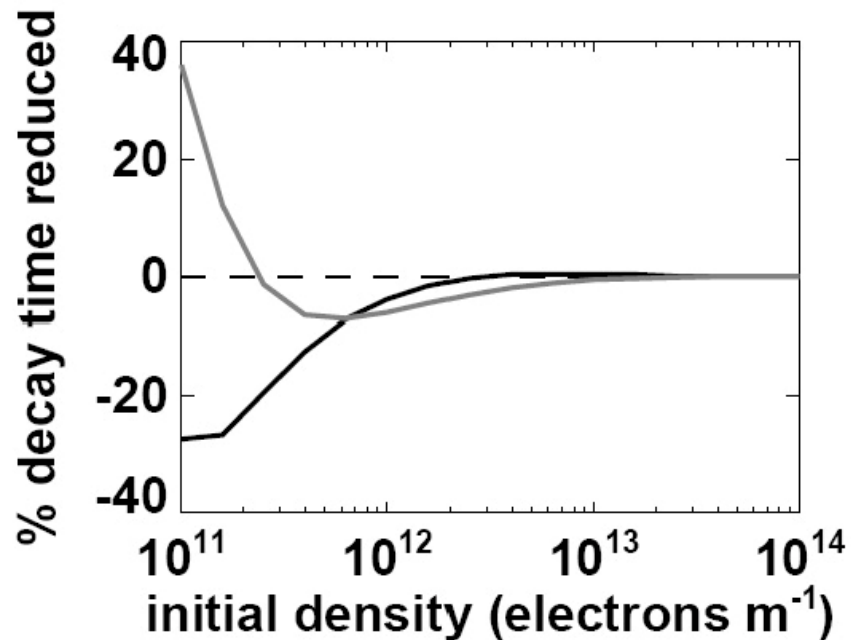


Havnes and Sigernes (2005), On the influence of background dust on scattering from meteor trails, *J. Atmos. Sol. Terr. Phys.*, 67, 659–664.

Jones, W. (1995), Theory of the initial radius of meteor trains, *Mon. Not. R. Astron. Soc.*, 275, 812-818.



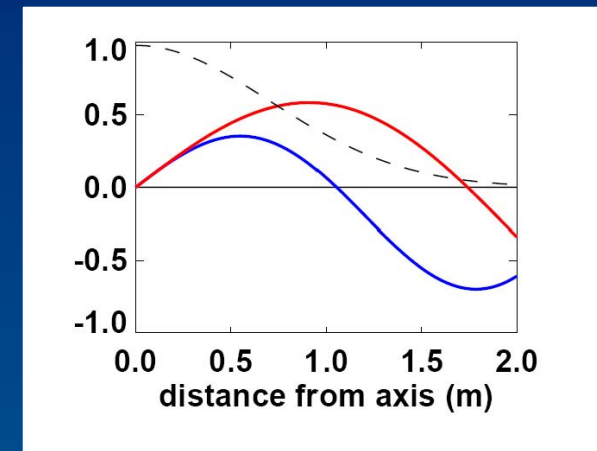
Model predictions



An example of the model predictions showing a reduction in decay times for 33 MHz (light) and 55 MHz (dark) radars for various trail densities. 1.0 m initial radius trail with aerosol parameters $n_d = 5 \times 10^9 \text{ m}^{-3}$ and $R_{ed} = 10^8 \text{ m}^3 \text{ s}^{-1}$.

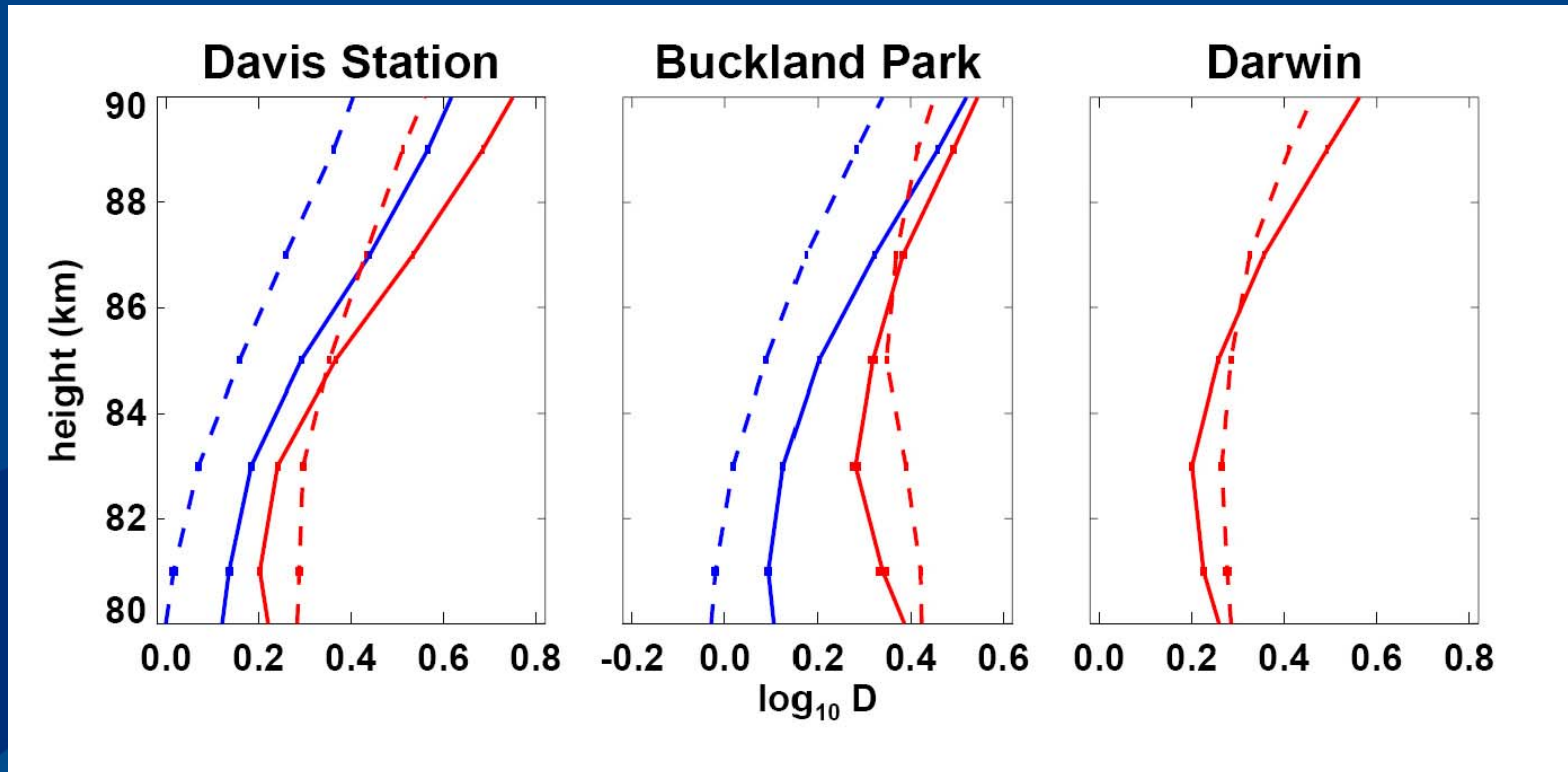
Note:

- Curves converge on expected value with an increase in initial line density
- 55 MHz decay times are increased for low line density values



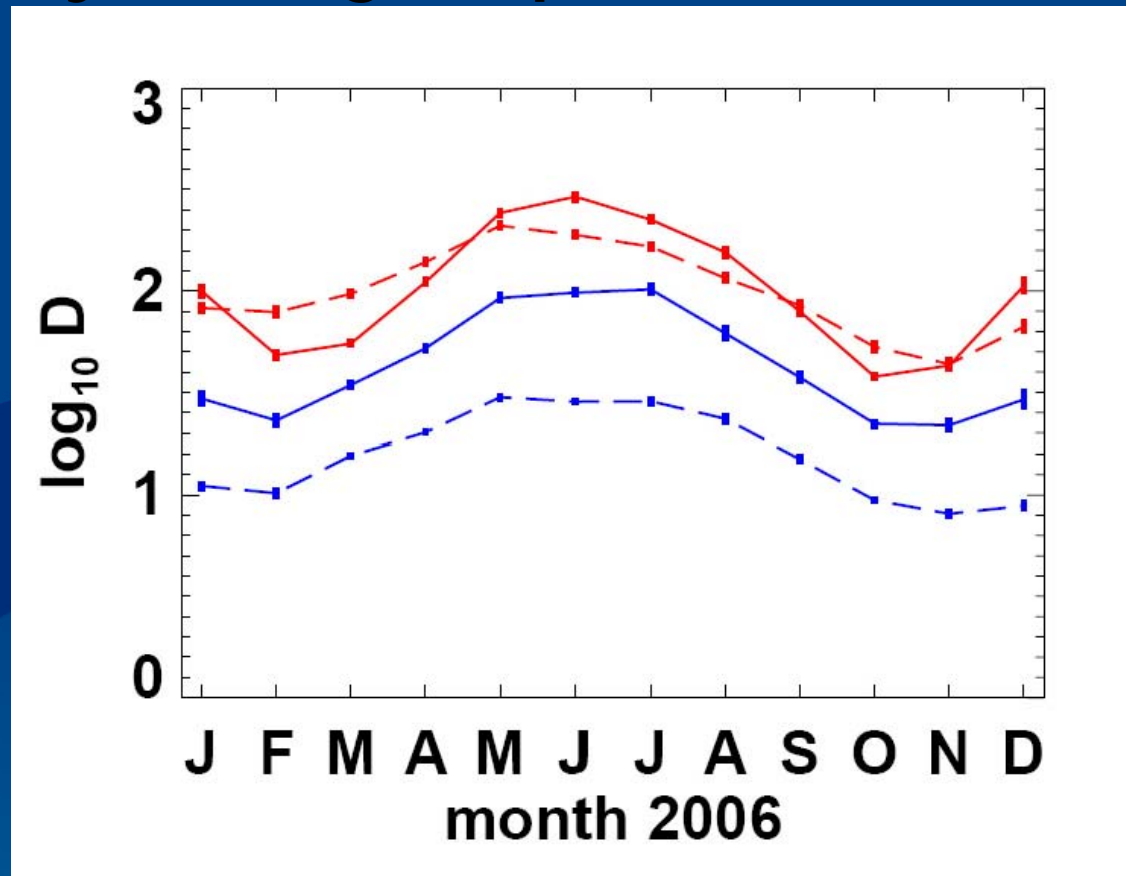
Weighting functions $rJ_0(4\pi r/\lambda)$ for 33 MHz (red) and 55 MHz (blue) radars. A Gaussian density profile with a 1.0 m radius (dashed) is shown for comparison.

Observations



Mean ambipolar diffusion coefficient estimates for March 2006 (October/September for Buckland Park 33 MHz): 25% weakest meteor echoes (dashed) and the 25% strongest meteor echoes (solid) using 33 MHz (red) and 55 MHz (blue) radars. Error bars are two standard errors.

Monthly average D plot for Davis



Red is 33 MHz radar and blue is 55 MHz. 25% strongest echoes are solid and 25% weakest are dashed. Error bars are two standard errors.

Conclusions



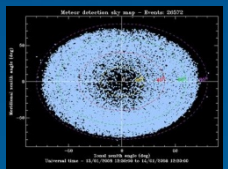
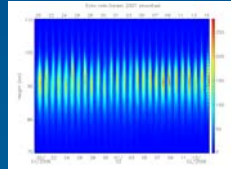
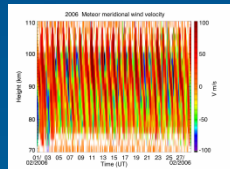
- All-sky meteor radars now a powerful tool for investigating winds and temperatures in the MLT region
- However, the “ambipolar diffusion coefficients” measured using the decay of meteor trails depend on echo strength and frequency
- Underdense meteors with low initial electron line density appear to be affected by absorptive processes related to the presence of dust and ice particles in the upper atmosphere
- Only higher power detections, corresponding to meteor trails with higher electron line densities, should be used to estimate atmospheric temperature and pressure
- The digi-TIGER radar has significant potential to contribute to studies of the MLT region in a custom meteor mode



Postscript: application of TIGER radars to MLT region studies



- *The dynamic behaviour of the MLT region between Australia and Antarctica*
 - **Significant atmospheric gravity wave source regions and generation mechanisms.** We will extend the *DAWEX* campaign approach to multiple sites (Darwin, Alice Springs, BP, the regions SE of BP and SW of both TIGER radar sites), allowing a detailed examination of the known generation region near Darwin and the propagation region between this source and Adelaide. Source regions over the Antarctic Continent and their northward propagation paths will become evident.
 - **Dominant atmospheric gravity wave scales, phase speeds, and momentum fluxes as a function of metrological conditions.** We have been able to contribute significantly to this topic in the past and the addition of the TIGER radar observations will significantly strengthen our capability in this area.
 - **Longer Term Observations.** Naturally, some investigations require a longer observing period. The Semi-Annual Oscillation (*SAO*), Annual Oscillation (*AO*) and Quasi-Biennial Oscillation (*QBO*) are all in this category. These oscillations are clearly evident in BP airglow intensity observations and in MF winds but many aspects of their interaction with each other, and with tidal and planetary scale waves, remains to be investigated.
 - **Climatologies.** Climatologies have been a by-product of our *ARC* funded research over many years. For example, as above, we have a continuous record of winds in the *60-100 km* height region from *1984*, continuous *OH* and *558 nm* airglow intensity since *1995*, *D-region* electron densities since *1995*, and continuous *OH* and *O2* spectrometer rotational temperature measurements dating to *2001*. These represent an extremely valuable resource as a background to case studies and in their own right as well as providing a climatological baseline. This project will allow this record to be extended and broadened and so mined for long term effects.



Acknowledgments.

Ray Morris and Damian Murphy of the Australian Antarctic Division are PIs on the Davis Station ST and meteor radars respectively and we acknowledge them for the use of these data. This research was supported by ASAC grant 2529 and ARC grants DP20049700 and DP450787.

